Aging Cell (2011) **10,** pp1067–1079 Doi: 10.1111/j.1474-9726.2011.00750.x

Conserved cysteine residues in the mammalian lamin A tail are essential for cellular responses to ROS generation

Vanja Pekovic,[1]* Ian Gibbs-Seymour,[1]* Ewa Markiewicz,[1] Fahad Alzoghaibi,[1] Adam M. Benham,[1] Robert Edwards,[1] Manfred Wenhert,[2] Thomas von Zglinicki[3] and Christopher J. Hutchison[1]

[1]School of Biological and Biomedical Sciences, Durham University, Durham DH1 3LE, UK
[2]Institute of Human Genetics, Ernst-Moritz-Arndt University, 17847 Greifswald, Germany
[3]Institute for Ageing and Health, Newcastle University, Newcastle-upon-Tyne NE4 5PL, UK

Summary

Pre-lamin A and progerin have been implicated in normal aging, and the pathogenesis of age-related degenerative diseases is termed 'laminopathies'. Here, we show that mature lamin A has an essential role in cellular fitness and that oxidative damage to lamin A is involved in cellular senescence. Primary human dermal fibroblasts (HDFs) aged replicatively or by pro-oxidants acquire a range of dysmorphic nuclear shapes. We observed that conserved cysteine residues in the lamin A tail domain become hyperoxidized in senescent fibroblasts, which inhibits the formation of lamin A inter- and intramolecular disulfide bonds. Both in the absence of lamin A and in the presence of a lamin A cysteine-to-alanine mutant, which eliminates these cysteine residues (522, 588, and 591), mild oxidative stress induced nuclear disorganization and led to premature senescence as a result of decreased tolerance to ROS stimulators. Human dermal fibroblasts lacking lamin A or expressing the lamin A cysteine-to-alanine mutant displayed a gene expression profile of ROS-responsive genes characteristic of chronic ROS stimulation. Our findings suggest that the conserved C-terminal cysteine residues are essential for lamin A function and that loss or oxidative damage to these cysteine residues promotes cellular senescence.

Key words: lamin A; aging; senescence; oxidative stress; redox homeostasis; laminopathies.

Introduction

Cellular senescence is a widely studied model for organismal aging (Campisi, 2005) and is thought to arise through chronic activation of stress responses to errors in DNA repair and oxidative damage (von Zglinicki *et al.*, 2003). At least two converging mechanisms lead to senescent arrest in human cells. Replicative senescence is a cell intrinsic mechanism apparently activated by critically short dysfunctional telomeres that are sensed as sites of DNA damage (d'Adda di Fagagna *et al.*, 2003; von Zglinicki *et al.*, 2005). Stress-induced premature senescence (SIPS) occurs in response to various stresses such as oxidative stress and non-telomeric DNA damage (Toussaint *et al.*, 2000; Gorbunova *et al.*, 2002).

According to the 'free radical theory of ageing', the balance between the production and elimination of intracellular reactive oxygen and/or nitrogen species (ROS/RNS) is a major determinant of cellular lifespan (Harman, 1956). The majority of cellular ROS is produced by mitochondria through aerobic respiration. Reactive oxygen and/or nitrogen species play important roles as intracellular signaling molecules, and they are not only involved in various cellular processes but also involved in pathogenesis of many age-related conditions. Excessive accumulation of ROS can lead to DNA damage and the buildup of irreversibly oxidized proteins. Therefore, mammalian cells are armed with many antioxidant defence mechanisms that eliminate excessive ROS and prevent accumulation of ROS-induced oxidative damage via protective response mechanisms. Some of these antioxidant defence systems include enzymes such as superoxide dismutase (SOD) and catalase (CAT) that catalyze the reduction of ROS as well as two major redox enzyme systems involving glutathione (GSH) and thioredoxin (Trx). ROS is also known to influence several transcription factors involved in stress signaling pathways such as Sp-1, AP-1, and NF-κB, which regulate the expression of stress response genes, including those encoding the major antioxidant enzymes (Haddad, 2002). Protective responses to excessive cellular ROS can also involve cells entering temporary growth arrest that allows time for repair of damaged DNA, regeneration of oxidized proteins and recovery of redox balance (Davies 1999). Cellular senescence, in contrast, is characterized by a permanent growth arrest, increased ROS levels, irreparable DNA damage, and a buildup of irreversibly oxidized proteins (von Zglinicki *et al.*, 2005; Friguet, 2006).

Recently, the *LMNA* gene has been linked to longevity and was proposed to be a guardian of somatic cells during their lifetime (Hutchison & Worman, 2004). Mutations in the *LMNA* gene cause a spectrum of age-related human diseases and progeroid syndromes including Hutchinson Gilford Progeria Syndrome (HGPS) and atypical Werner syndrome (AWS) (Worman & Bonne, 2007). These diseases, collectively termed 'laminopathies', affect the maintenance of one or more tissues of mesenchymal origin. In addition, mouse models of laminopathies have shortened lifespans (Stewart *et al.*, 2007), and down-regulation of Ce-lamin in *Caenorhabditis elegans* also leads to a decrease in lifespan (Haithcock *et al.*, 2005).

The nuclear lamins are type V intermediate filament proteins of A-type and B-type that form a stress-resistant network of filaments underneath the inner nuclear membrane (Broers *et al.*, 2006). Lamin monomers consist of an alpha-helical rod domain flanked by a N-terminal head domain and a C-terminal globular tail, and become assembled in the nucleus through dimerization, polymerization, and higher-order assembly (Stuurman *et al.*, 1998; Ben-Harush *et al.*, 2009). B-type lamins are encoded by two distinct genes, *LMNB1* and *LMNB2*, and are essential for cell survival (Harborth *et al.*, 2001) and appear to have interchangeable but essential functions in embryogenesis (Vergnes *et al.*, 2004). A-type lamins include two major isoforms, lamins A and C, produced by alternative splicing of the *LMNA* gene and are essential for post-natal development and differentiation (Broers *et al.*, 2006). In addition to providing structural support to the nucleus, the nuclear lamins are involved in transcriptional silencing (Reddy *et al.*, 2008), cell cycle control (Johnson *et al.*, 2004; van Berlo *et al.*, 2005; Pekovic *et al.*, 2007), DNA repair (Liu *et al.*, 2005), and signal transduction (Pekovic & Hutchison, 2008).

Correspondence
Dr Chris Hutchison, The School of Biological and Biomedical Sciences, The University of Durham, Durham DH1 3LE, UK. Tel.: +0044 191 334 1270; fax: +0044 191 334 1201; e-mail: c.j.hutchison@durham.ac.uk

*The first two authors contributed equally to this work.

Accepted for publication *16 September 2011*

© 2011 The Authors
Aging Cell © 2011 Blackwell Publishing Ltd/Anatomical Society of Great Britain and Ireland

Aging Cell

Mature lamin A is synthesized as a precursor pre-lamin A containing an isoprenylation signal at its C-terminus, the C-cysteine; A-any aliphatic amino acid; X-any amino acid motif (CAAX) (Rusinol & Sinensky, 2006). This motif undergoes a sequence of modifications that includes the final removal of the C-terminal modified cysteine. Mutations in the pre-lamin A processing enzyme Zmpste24/FACE1 lead to an accumulation of pre-lamin A precursors and result in premature aging diseases (Navarro *et al.*, 2004). In HGPS, splice site mutations in the *LMNA* gene lead to production of a truncated pre-lamin A protein named 'progerin', which cannot undergo the final processing step and thus becomes permanently farnesylated (Cao *et al.*, 2007; Dechat *et al.*, 2007). One of the hallmarks of patient cells expressing progerin or pre-lamin A includes deformations in nuclear morphology and a decreased proliferative potential (Bridger & Kill, 2004; Goldman *et al.*, 2004; Espada *et al.*, 2008).

Lamin A variants have recently been implicated in normal cellular and tissue aging. Abnormal nuclear shapes and low levels of progerin are present in fibroblasts and skin tissue of old individuals (McClintock *et al.*, 2006, Scaffidi & Misteli, 2008). In addition, pre-lamin A accumulation has also been reported during cellular senescence (Ukekawa *et al.*, 2007; Candelario *et al.*, 2008, Huang *et al.*, 2008). Interestingly, reports have also shown a decreased expression of lamin A in different cell types of old mice (Duque & Rivas, 2006). These studies suggest that a number of mechanisms could be at work by which pre-lamin A may influence cellular senescence. However, no study so far has addressed what role, if any, mature lamin A plays in cellular senescence. Here, we show that conserved cysteine residues in the lamin A tail domain are targets for irreversible oxidative damage during replicative senescence. Furthermore, we show that in the absence of lamin A or following the loss of the conserved cysteine residues, basal levels of cellular ROS are elevated and following only mild levels of ROS stimulation cells enter a state of senescence prematurely. Our findings suggest that the conserved cysteine residues in the lamin A tail are essential ROS-related functions of lamin A.

Results

Senescence-associated hyperoxidation of cysteine residues in the lamin A tail

Human dermal fibroblasts (HDFs) that have been aged in culture display a range of dysmorphic nuclear shapes that are reminiscent of those observed in fibroblasts from patients with HGPS (data not shown). Previous studies have shown that oxidative damage during cellular aging can lead to protein unfolding (Friguet, 2006) and that protein thiols are prime targets of oxidative modifications (Eaton, 2006). We thus investigated whether lamin A could be a target of oxidative thiol damage in senescent HDFs, which could, in turn, contribute to the accumulation of dysmorphic nuclei. Multiple sequence alignments of lamins A, C, B1, and B2 revealed that lamin A contains three unique cysteine residues (C570, C588, and C591) in its specific C-terminal tail and shares a single surface–exposed cysteine residue (Krimm *et al.*, 2002) with lamin C in the common IgG domain (C522) (Fig. S1, Supporting information). None of these cysteine residues are present in lamins B1 or B2. Three cysteines (C522, C588, and C591) are conserved throughout the mammalian phylogeny (Fig. S2, Supporting information). Interestingly, while C522 is not found in non-mammalian vertebrates, C588 and C591 are conserved in all vertebrates.

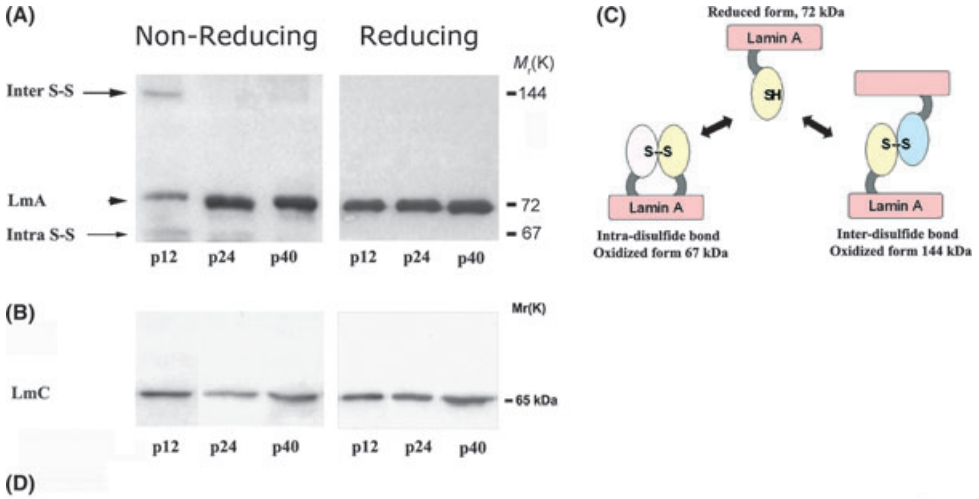
Cysteine residues in proteins can form disulfide bonds under oxidizing conditions, which can be detected on non-reducing SDS-PAGE as slower-migrating protein species in the case of intermolecular disulfide bonds or faster-migrating protein species in the case of intramolecular disulfide bonds (Benham *et al.*, 2000). To investigate potential disulfide bond formation during senescence, HDFs at different population doublings (p12, p24, and p40) were *N*-ethylmaleimide (NEM)-treated, extracted, and resolved on non-reducing or reducing SDS-PAGE and probed with antibodies that detect lamin A (Jol4) and C (RalC) individually. Under non-reducing conditions, lamin A was weakly detected as a monomer at p12 but exhibited two band shifts to the positions of slower-migrating and faster-migrating protein species. Under reducing conditions, lamin A was detected only as a monomer across all three population doublings (Fig. 1A), confirming that both the slower- and the faster-migrating bands of lamin A in p12 HDFs were disulfide dependent. In contrast, we observed a progressive decline in the amounts of both inter- and intramolecular disulfide species with increasing population doublings resulting in the accumulation of lamin A monomers at p40 (Fig. 1A and C). Lamin C, in contrast, migrated as a monomer across all three passages under both non-reducing and reducing conditions (Fig. 1B). Control extracts prepared in the absence of NEM gave similar results in the high and low molecular weight disulfide forms of lamin A in early-passage HDF, indicating that the disulfide bonds did not form post-lysis (data not shown). These findings suggest that the cysteine residues in the lamin A tail promote both inter- and intradisulfide bond formation. With increased replicative age, cysteine residues in lamin A become progressively less available for forming disulfide bonds.

Protein thiols can undergo different degrees of oxidation, which can be either reversible (sulfenic acid) or irreversible (sulfinic and sulfonic acids) (Eaton, 2006). To find out whether cysteine residues in lamin A become irreversibly oxidized in senescent HDFs, we applied MALDI-TOF/TOF peptide mass fingerprinting in conjunction with reductive thiol-trapping alkylation. The results are summarized in Fig. 1D and shown in Fig. S3 (Supporting information). Three cysteine-containing peptides of lamin A were identified in the Mascot database: αα516-27, which contains C522, and αα585-97 and αα583-97 (the latter having one missed cleavage site at R585), both containing C588 and C591. We found that at p12, the observed and predicted masses of each peptide corresponded to the mass difference of either one (αα516-27) or two (αα583-97 and αα585-97) alkylation adducts, indicating an absence of reduction-resistant oxidative modifications. In contrast, at p40 the observed and predicted peptide masses differed by 32 Da (αα516-27) or 48 Da + a mass of one alkylation adduct (αα583-97 and αα585-97). The observed peptide modifications were resistant to DTT reduction and corresponded to those expected for irreversible oxidation to sulfinic (SO_2H) and sulfonic (SO_3H,) acids, respectively. Thus, in senescent HDFs, lamin A cysteines were irreversibly oxidatived, potentially explaining their decreased ability to form disulfide bonds under oxidizing conditions.

Temporary cell cycle arrest of human dermal fibroblast in response to mild oxidative stress is correlated with disulfide bond formation in lamin A

It has been proposed that the formation of disulfide bonds is part of a protective response to mild oxidative stress (Eaton, 2006). Human dermal fibroblasts enter a state of SIPS following exposure to ROS. While a high-level exposure to pro-oxidants induces SIPS, mild oxidative stresses elicit a protective stress response leading to temporary growth arrest (Davies, 1999). Hydrogen peroxide (H_2O_2) is the most widely used pro-oxidant as it is produced physiologically and serves as an essential second messenger in redox signaling (Toussaint *et al.*, 2000). As we showed that lamin A forms disulfide bonds in young HDFs but not in senescent HDFs, we investigated whether lamin A forms disulfide bonds in response to H_2O_2. Based on our findings (Fig. 1) and the proposals of Davis *et al.* and Eaton, we anticipated that mild exposure to H_2O_2 would lead to temporary cell

© 2011 The Authors
Aging Cell © 2011 Blackwell Publishing Ltd/Anatomical Society of Great Britain and Ireland



(D)

PDL	Residue number	Observed mass	Predicted mass	Δ mass	Sequence	Modification
p12	516-527	1431.6	1306.6	125	K AQNTWGCGNSL R	NEM
p40	516-527	1338.6	1306.6	32	K AQNTWGCGNSL R	SO_2H
p12	583-597	1785.7	1535.7	250	R SRTVLCGTCGQPAD K	2 x NEM
p40	583-597	1708.7	1535.7	173	R SRTVLCGTCGQPAD K	NEM + SO_3H
p12	585-597	1542.6	1292.6	250	R TVLCGTCGQPAD K	2 x NEM
p40	585-597	1465.6	1292.6	173	R TVLCGTCGQPAD K	NEM + SO_3H

Fig. 1 Hyperoxidation of lamin A tail thiol residues in senescent fibroblasts. Protein extracts from p12-40 human dermal fibroblasts (HDFs) were subjected to non-reducing or reducing SDS-PAGE and immunoblotted against JoL4 (A) to detect lamin A or RaLC (B) to detect lamin C. Thick arrow, lamin A (72 kDa); thin arrow, lamin A intramolecular disulfide (~ 67 kDa). *, Lamin A intermolecular disulfide (~ 144 kDa). (C) Cartoon showing redox-dependent formation of lamin A intra- and intermolecular disulfides (S-S) Note the intermolecular bonds could form with other lamin A polypeptides or with other lamin A binding proteins (e.g., LAP2α). SH, cysteine sulfhydryl group. (D) MALDI-TOF/TOF peptide mass fingerprinting of lamin A peptides isolated from p12 and p40 HDF in the presence of *N*-ethylmaleimide. Three lamin A cysteine-containing peptides αα516-27 (C522), αα583-97, and αα585-97 (C588 and C591) were identified in Mascot database (C570-containing peptide was not detected and could not be analyzed). The mass differences (in daltons) between observed and predicted peptide mass peaks, the amino acid sequence of modified peptides, and their corresponding modifications are listed. SO_2H, sulfinic acid; SO_3H, sulfonic acid.

cycle arrest and the formation of lamin A disulfide bonds, whereas excessive doses of H_2O_2 would cause entry into a senescent state, in part by inhibiting the formation of lamin A disulfide bonds.

We first investigated the growth of HDF in the presence of either low or high levels of H_2O_2. Early-passage HDFs were treated *in vivo* with either 150 or 350 μM H_2O_2 alone, or following antioxidant pre-treatment with *N*-acetyl cysteine (NAC) (Fig. 2A). The viability of HDFs was not affected by any of the treatments (not shown). Following the treatments, cells were either cultured for 72 h or were reseeded and cultured for 24 h, and then assessed for cellular morphology, expression of proliferation markers, expression of senescence-associated (SA)-β-gal activity, and nuclear morphology. In response to 150 μM H_2O_2 alone, HDFs entered a state of growth arrest, demonstrated by reduced expression of the proliferation marker Ki67 (< 30% cells were Ki67-positive Fig. 2B). The growth arrest was readily reversible following reseeding in the absence of H_2O_2, as assessed by a spindle-shaped cell morphology (Fig. 2A) and a high Ki67+ index (> 70% cells were Ki67-positive, Fig. 2B). Treatment of HDF with 150 μM H_2O_2 did not affect nuclear morphology (Fig. 2E) or induce expression of β-gal (Fig. 2D). In contrast, in response to 350 μM H_2O_2, HDFs entered a state of SIPS as shown by a flattened cell morphology (Fig. 2A), greatly reduced Ki67 labeling (< 20%, Fig. 2C) and high SA-β-gal activity (> 50%, Fig. 2D). None of these phenotypes was reversed by reseeding in the absence of H_2O_2. Premature entry into a senescent state was correlated with greatly increased numbers of abnormally shaped nuclei (Fig. 2E). Pre-treatment of HDFs with the free radical scavenger NAC prevented both the transient effects of 150 μM H_2O_2 and the senescence-inducing effects of 350 μM H_2O_2 (Fig. 2A–E, Fig. S4, Supporting information).

To analyze the redox state of lamin A in response to oxidative stress, p12 HDFs were treated with either 150 μM or 350 μM H_2O_2 *in vivo*. Cell extracts were prepared in the presence of the alkylating agent NEM and resolved on non-reducing or reducing SDS-PAGE. In untreated cells, both faster- and slower-migrating forms of lamin A were weak but detectable with JoL4 (Fig. 2F). The detection of the faster- and slower-migrating bands increased significantly after treatment with 150 μM H_2O_2, suggesting enhanced intradisulfide and interdisulfide bond formation in response to mild oxidation. Neither species was detected in the presence of 350 μM H_2O_2, suggesting that thiol residues were unavailable for disulfide bond formation (Fig. 2F). Under reducing conditions, lamin A was detected as a monomer after each H_2O_2 treatment (Fig. 2F lower) confirming that the slower and faster-migrating species were disulfide dependent. Importantly, following NAC pre-treatment, there was neither an increase in the level of disulfide bond formation in the presence of 150 μM H_2O_2 nor any elimination of disulfides following 350 μM H_2O_2 (Fig. S4C, Supporting information). Taken together, these findings show that in response to

© 2011 The Authors
Aging Cell © 2011 Blackwell Publishing Ltd/Anatomical Society of Great Britain and Ireland

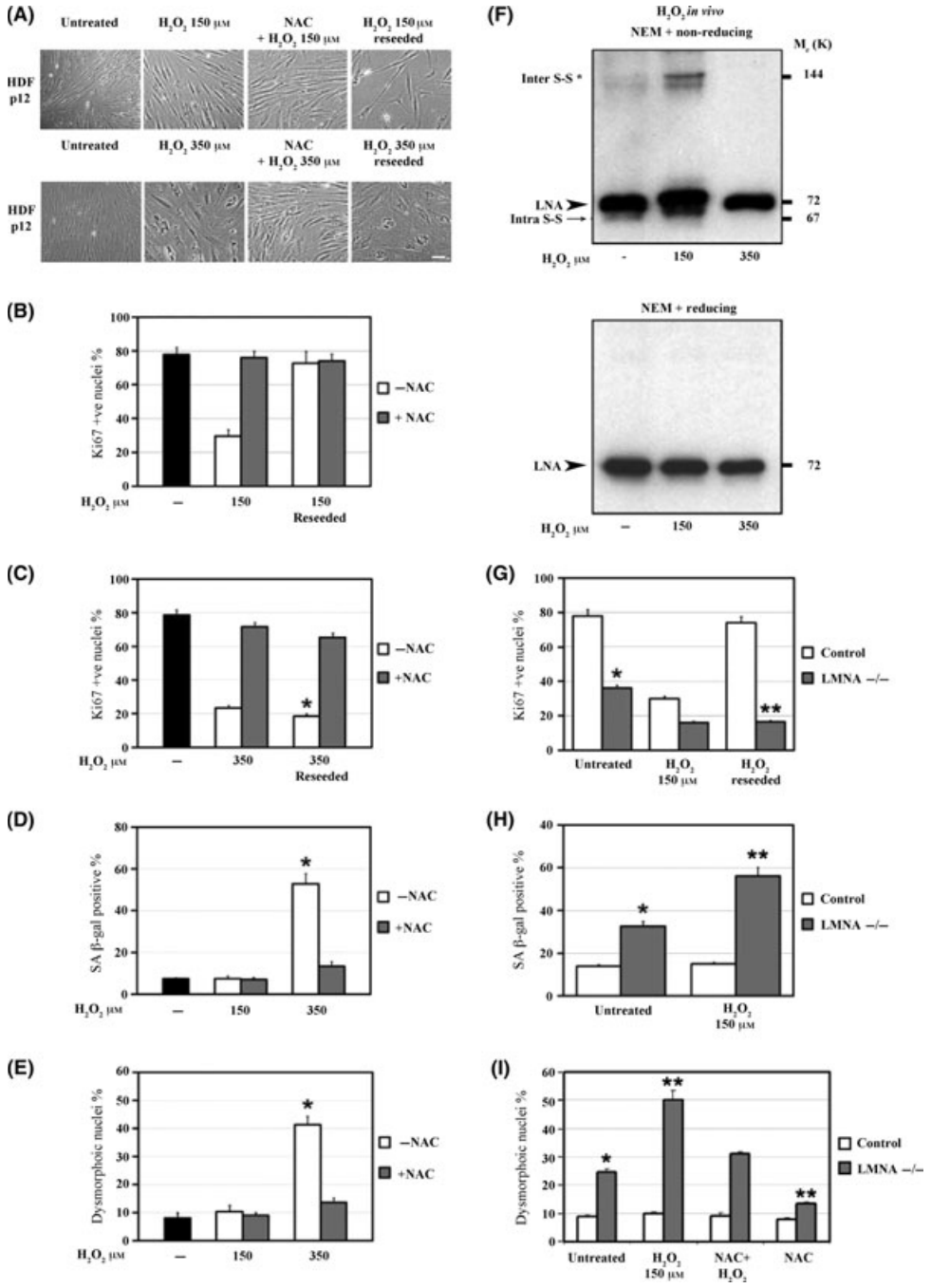


Fig. 2 The effects of oxidative stress on lamin A disulfide bond formation, nuclear morphology, and cell proliferation. (A–E) human dermal fibroblasts (HDFs) p12 were either left untreated or treated with 150 μM or 2 × 350 μM H_2O_2 in the presence or absence of 10 mM *N*-acetyl cysteine (NAC). (A) Phase contrast images of cells of untreated, H_2O_2 stimulated, or reseeded cells. Scale bar = 20 μm. (B) The fraction of Ki67-positive cells before and after reseeding following treatments with 150 μM H_2O_2 +/− 10 mM NAC. (C) The fraction of Ki67-positive nuclei before and after reseeding following treatments with 2 × 350 μM H_2O_2 +/− 10 mM NAC. Black bar = untreated cells. (D) The fraction of senescence-associated (SA)-β-gal-positive cells and (E) dysmorphic nuclei after reseeding following H_2O_2 treatments +/− 10 mM NAC. (F) Protein extracts from untreated, 150 and 2 × 350 μM H_2O_2-treated HDFs were prepared with 40 mM *N*-ethylmaleimide, resolved on non-reducing/reducing SDS-PAGE and probed with JoL4. Thick arrow, lamin A (72 kDa); thin arrow, lamin A intramolecular disulfide (~ 67 kDa); *, lamin A dimer (~ 144 kDa). (G – I) Control and Y259X (lamin A/C –/–) HDFs were left untreated or treated with 150 μM H_2O_2 and the fraction of Ki67-positive cells (G), SA-β-gal-positive cells (H) and dysmorphic nuclei (I) determined before (G) and after reseeding (G–I). Fractions were calculated by scoring 300 cells from random fields on triplicate coverslips in three independent experiments. Means ± SD are shown. *P < 0.05 relative to 150 μM H_2O_2-treated HDFs without NAC (C–E). *P < 0.05, **P < 0.01 compared to untreated control HDF (G,H). *P < 0.05 compared to untreated control HDF, or **P < 0.01 compared to untreated Y259X HDF.

mild oxidative stresses HDFs enter a state of temporary cell cycle arrest and that this is correlated with the formation of disulfide bonds in lamin A. However, in the absence of effective ROS scavenging, high levels of oxidative stress promote SIPS and this is correlated with the appearance of dysmorphic nuclei and absence of disulfide bond formation in lamin A.

© 2011 The Authors
Aging Cell © 2011 Blackwell Publishing Ltd/Anatomical Society of Great Britain and Ireland

Human dermal fibroblasts are hypersensitive to ROS stimulation in the absence of lamin A

Our data have thus far correlated entry into a senescent state with oxidation of C-terminal cysteine residues and/or loss of the ability to form inter- and intradisulfide bonds in lamin A. Senescence is also correlated with the appearance of dysmorphic nuclei, suggesting the presence of non-functional lamin A. To determine the role of lamin A in cellular senescence, we investigated the cellular response to mild oxidative stress in HDFs harboring a homozygous mutation Y259X in the *LMNA* gene, which are null for expression of lamins A/C (Muchir *et al.*, 2003). We hypothesized that in the absence of lamin A, these HDFs would be more sensitive to mild oxidative stresses and thus have an increased likelihood of undergoing SIPS instead of temporary growth arrest. Wild-type and Y259X HDFs were either left untreated or treated *in vivo* with 150 μM H_2O_2 and analyzed for their proliferative capacity, expression of SA-β-gal, and nuclear morphology. As observed previously (Pekovic *et al.*, 2006), Y259X HDFs showed a reduced Ki67 proliferative index and an increased proportion of cells having dysmorphic nuclei and SA-β-gal expression as compared to wild-type HDFs under standard growth conditions (Fig. 2G–I). In response to 150 μM H_2O_2, wild-type HDFs entered a growth arrest as shown by a ~ 2.5-fold reduction in expression of Ki67, but re-entered the cell cycle following reseeding as shown by re-expression of Ki67 (Fig. 2G). Treatment of wild-type HDFs with 150 μM H_2O_2 did not induce either SA-β-gal expression or the appearance of dysmorphic nuclei (Fig. 2H,I). In contrast, treatment of Y259X HDFs with 150 μM H_2O_2 led to a 2-fold reduction in Ki67 expression, which was not reversible following reseeding (Fig. 2G), and caused them to enter SIPS as shown by a > 2.0-fold increase in both SA-β-gal activity and the percentage of dysmorphic nuclei (Fig. 2H,I). To test whether the presence of dysmorphic nuclei in Y259X fibroblasts was directly linked to oxidative stress, we treated the fibroblasts with the ROS chelator NAC in the presence or absence of H_2O_2. Both the basal fraction of cells and H_2O_2 induced fraction of cells having dysmorphic nuclei were reduced ~ 2-fold following NAC pretreatment (Fig. 2I). Based on these results, it appears that lamin A has an essential role in an adaptive response to oxidative stress.

Loss of conserved C-terminal lamin A cysteine residues abrogates lamin A function in an adaptive response to oxidative stress and promotes cellular senescence

Our data thus far have revealed that lamin A is essential for an adaptive response to oxidative stress and that entry into a senescent state is correlated with oxidation of conserved cysteine residues in the lamin A tail domain. Moreover, the adaptive response of HDF to mild oxidative stress is correlated with the formation of inter- and intramolecular disulfide bonds in lamin A. To test the hypothesis that redox-dependent lamin A disulfide bond formation is part of an adaptive response to oxidative stress, we used site-directed mutagenesis to produce cysteine-to-alanine Flag-tagged lamin A constructs including the single mutants C552A, C588A, C591A, a double mutant C588/591A, and a triple mutant C522/588/591A. Wild-type and mutant constructs were expressed in p12 HDFs, and cell extracts, prepared in the presence of NEM, were resolved on non-reducing or reducing SDS-PAGE and probed with anti-FLAG antibody or JoL4 (not shown). The anti-FLAG antibody detected a non-specific band migrating ~ 60 kDa even in untransfected HDF (Fig. 3A). Under non-reducing conditions, Flag-wt lamin A was detected as a monomer as well as the slower- and faster-migrating protein bands, indicating the formation of both inter- and intramolecular disulfide bonds. Mutants C588A, C591A, and C522A also formed inter- and intramolecular disulfide bonds. Interestingly, for mutants C522A and C588A multiple slower-migrating bands were observed (Fig. 3A), implying that these mutants permitted intermolecular disulfide bond formation between more than one lamin A binding partner (Fig. 3A + symbols in gel). In addition for all three mutants, the Mr of the faster-migrating bands differed from wild-type lamin A (Fig. 3A) presumably because different intradisulfides were formed. Both intra- and intermolecular disulfide bonds were very weak or undetectable in the double (C588/591A) mutant (Fig. 3A). All disulfide bond formation was undetectable in the triple mutant (C522/588/591A) (Fig. 3A) even when the gels were overexposed (not shown). As expected, all Flag-lamin A proteins migrated as monomers under reducing conditions (Fig. 3B). Together, these mutants provide tools to investigate firstly, whether some or all of the conserved cysteine residues are necessary for cellular resilience to ROS and second whether disulfide bond formation is a component of an adaptive cellular response to oxidative stress.

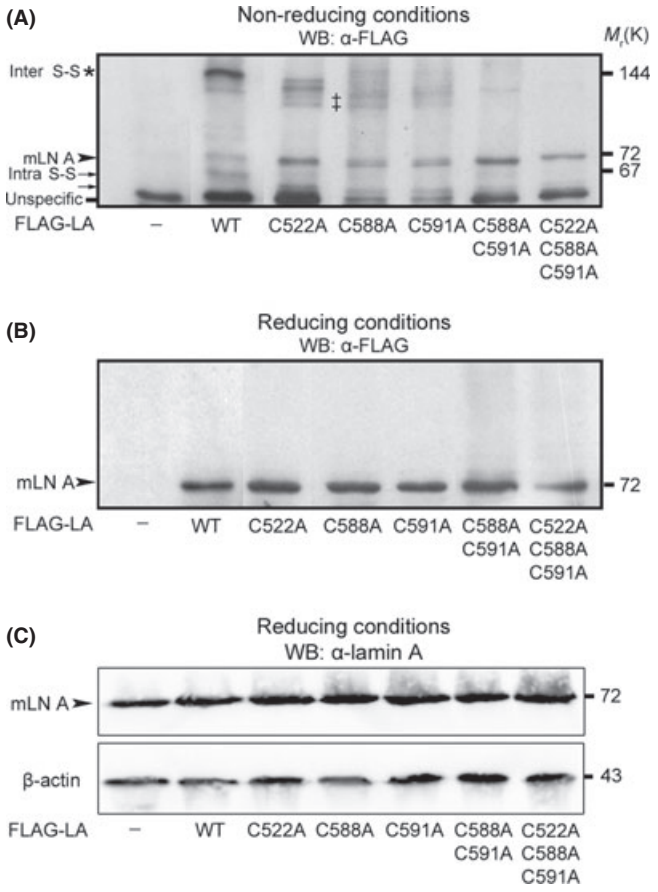


Fig. 3 The effects of Cysteine-Alanine mutations in the ability of lamin A to form disulfide species. (A,B) Human dermal fibroblasts (HDFs) were transfected with Flag-wt or one of five different Flag-cys-ala lamin A constructs. Protein extracts prepared in the presence of *N*-ethylmaleimide were resolved on non-reducing (A) or reducing (B) SDS-PAGE and probed with FLAG M2 antibodies. Lanes contain untransfected control (–), wild-type lamin A (WT), C522A, C588A, C591A single-lamin A mutants, C588/591A double-lamin A mutants, or C522/588/591A triple-lamin A mutants. Arrowhead, lamin A monomer; arrow intramolecular disulfide species; *, intermolecular disulfides species. HDF were transfected with the same constructs and probed with anti-lamin A (1332A) or anti-β-actin antibodies. Chart shows fold expression of cys-ala lamin A protein relative to endogenous lamin A in untransfected control and normalized to β-actin following optical densitometry (C).

© 2011 The Authors
Aging Cell © 2011 Blackwell Publishing Ltd/Anatomical Society of Great Britain and Ireland

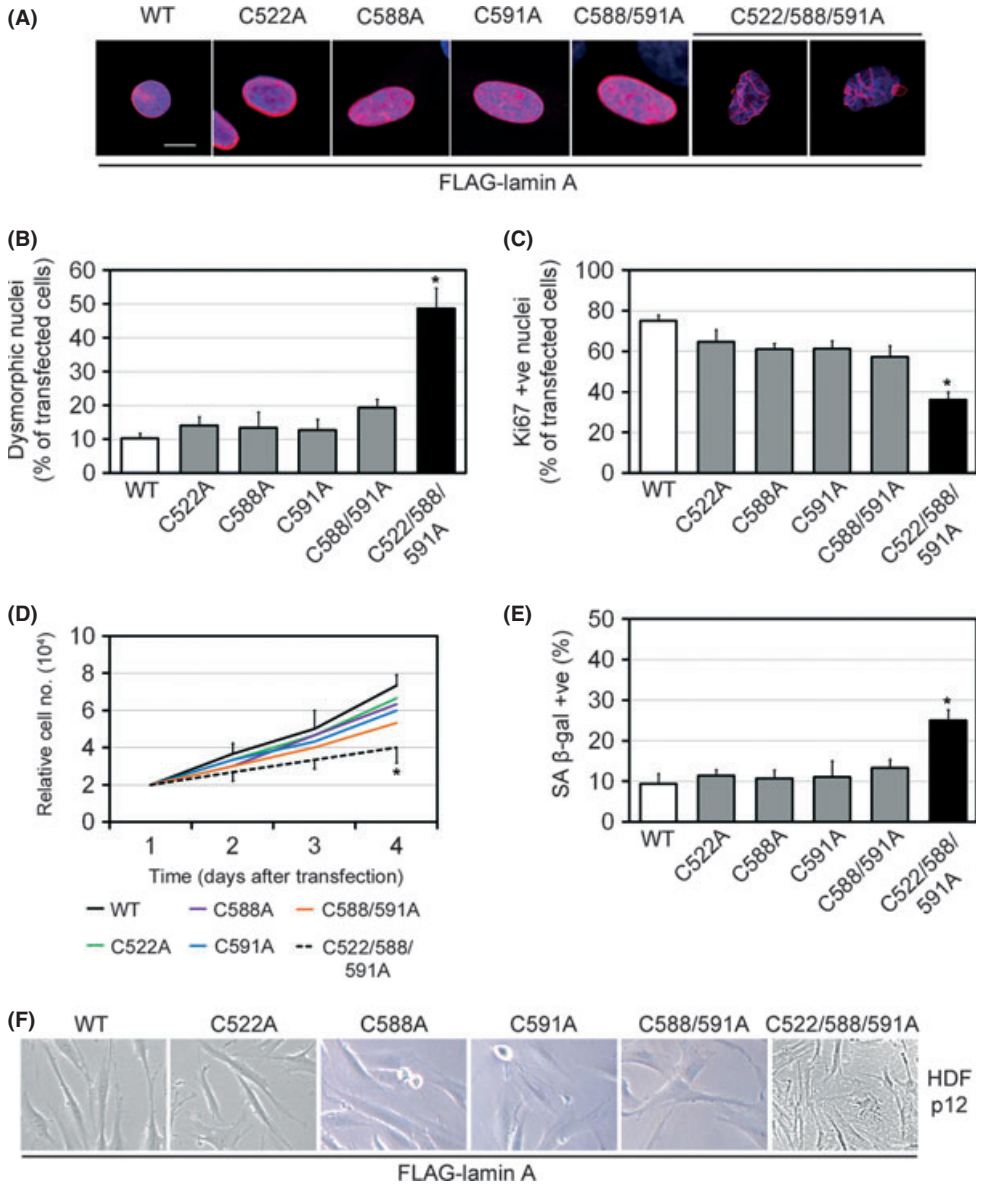


Fig. 4 A triple-lamin A mutants C522/588/591A impair cellular fitness causing premature senescence. (A) Human dermal fibroblasts (HDFs) (p12) were transfected with Flag-wt (WT) or one of C522A, C588A, C591A, C588/591A, or C522/588/591A mutant lamin A constructs and co-stained with FLAG M5 and 4,6-diamidino-2-phenylindole (DAPI). Micrographs are displayed as two-color merged images (FLAG, red; DAPI, blue). Scale bar = 10 μm. The fraction of FLAG positive cells showing dysmorphic nuclei (B) or Ki67-positive cells (C) for each construct used. Fractions were calculated by counting 300 cells from triplicate coverslips in three independent experiments. *$P < 0.05$ compared to WT HDF. (D) Growth curves of cells transfected with WT or each of the cys-ala lamin A mutants. Growth curves were calculated by estimating the number of cells recovered each day from duplicate 35-mm dishes in triplicate experiments. *$P < 0.05$. (H) The fractions of senescence-associated (SA)-β-gal-positive transfected HDFs were calculated by counting 300 cells in triplicate wells in three independent experiments. *$P < 0.05$. (i) Phase contrast images of Flag-wt, Flag-C522A C588A, C591A, C588/591A or C522/588/591A mutant lamin A transfected HDFs. Scale bars = 20 μm.

To examine the effects of cys-ala lamin A mutants on nuclear morphology and cell proliferation, early-passage HDFs were transfected with Flag-wild-type (Flag-wt) lamin A and each of the lamin A mutants individually. The level of over-expression of lamin A was then investigated by immunoblotting with JoL4. The results indicated that on average there was a 1.5- to 2.0-fold increase in the level of lamin A following transfection (quantified by densitometry), suggesting an approximate 1:1 ratio of endogenous compared to Flag-lamin A (Fig. 3C). As expected, Flag-wt lamin A localized both to the nuclear envelope and to the nucleoplasm and > 85% of transfected HDFs showed normal nuclear morphology (Fig. 4A). Each of C552A, C588A, and C591A also localized strongly to the nuclear envelope, and transfected HDF displayed normal nuclear morphology (Fig. 4A). C588/591A also localized to the nucleus but displayed elevated levels of nuclei containing aggregates of flag-tagged proteins (~ 20% of transfected cells) (Fig. 4A). In contrast, the triple mutant (C522/588/591A) was grossly disorganized within the nuclei, and ~ 45% of transfected HDFs displayed dysmorphic nuclear shapes (Fig. 4A,B). The proliferative capacity of transfected cells also differed depending on which mutant was expressed. The proliferation index (measured with Ki67) and the growth rates in HDF did not differ significantly

© 2011 The Authors
Aging Cell © 2011 Blackwell Publishing Ltd/Anatomical Society of Great Britain and Ireland

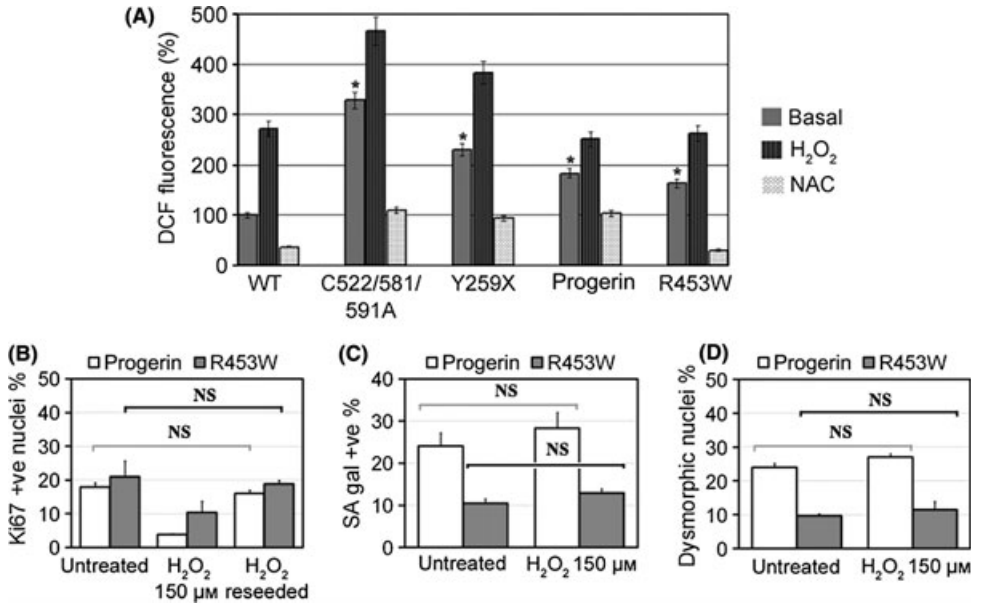


Fig. 5 C522/588/591A lamin A mutants impair ROS homeostasis. (A) Human dermal fibroblasts (HDFs) transfected with Flag-wt or C522/588/591A lamin A together with patient HDFs that are null for lamin A/C (Y259X), express progerin or express an Autosomal dominant Emery Dreifuss Muscular Dystrophy (AD-EDMD) mutation R453W were measured for intracellular ROS levels by flow cytometric tracing of relative dichlorofluorescein (DCF) fluorescence in untreated cells (basal), following treatment with 150 μM H_2O_2 or after antioxidant treatment with 10 mM *N*-acetyl cysteine (NAC). Dichlorofluorescein fluorescence is expressed as % relative to Flag-wt HDFs or control HDFs (not shown), which is set at 100%. The increase or decrease in DCF fluorescence following H_2O_2 or NAC treatments, respectively, is expressed as % relative to the basal level for each culture. Means ± SD are shown. *$P < 0.05$ compared to Flag-wt HDFs or control HDFs. (B–D) Patient HDFs expressing progerin or AD-EDMD mutation R453W were left untreated or treated with 150 μM H_2O_2 and the fractions of Ki67-positive cells (B), senescence-associated (SA)-β-gal-positive cells (C) and dysmorphic nuclei (D) determined before (B) and after reseeding (B–D). Fractions were calculated by scoring 300 cells from random fields on triplicate coverslips in three independent experiments. Means ± SD are shown. NS, not significant when comparing untreated cells with 150 μM H_2O_2-treated cells after reseeding for each culture.

following transfection with wt, C522A, C588A, or C591A Flag-lamin A (Fig. 4C,D). Transfection with C588/591A did not affect the proliferation index (Fig. 4C) but did impair the growth rate of HDF although this impairment did not reach statistical significance (Fig. 4D). Finally, transfection with the triple mutant C552/588/591A significantly reduced the proliferation index (to < 40%) and halved the growth rate of HDF when compared to transfection with both the wild-type Flag-lamin A and the single mutants (Fig. 4C,D). When we investigated the emergence of a senescent phenotype, either by expression of β-gal (Fig. 4E) or by cell morphology (Fig. 4F), only the triple mutant (C522/588/591A) was able to induce cellular senescence in a significant fraction (> 25%) of fibroblasts. Overall, these experiments have yielded two important results. Firstly, the ability to form disulfide bonds is not directly linked to entry into a senescent state, because the C588/591A (in which disulfide bond formation is almost absent) does not induce a senescent phenotype. Second, the loss of all three C-terminal cysteine residues generates a phenotype that is remarkably similar to a lamin A null phenotype, suggesting that these three cysteine residues are essential for lamin A function in preventing stress-induced senescence.

The presence of C522/588/591A and absence of lamin A both cause ROS intolerance in human dermal fibroblasts

To further investigate the hypothesis that the lamin A mutants C552/588/591A abrogate lamin A function in preventing stress-induced senescence, we compared ROS generation in HDF expressing mutant C552/588/591A or Flag-wt lamin A or in the following patient cell lines: lamin A null fibroblasts (Y259X), HGPS fibroblasts expressing progerin, and HDF expressing a milder mutant R453W that promotes Autosomal dominant Emery Dreifuss Muscular Dystrophy (AD-EDMD).

Human dermal fibroblasts were treated with 150 μM H_2O_2, and the levels of ROS before or after treatment were determined using a ROS-sensitive fluorescent dye (Eruslanov & Kusmartsev, 2010). We found that in HDF expressing mutant C522/588/591A, basal levels of ROS were 3-fold higher when compared to HDFs expressing Flag-wt (Fig. 5A). The presence of single-lamin A mutants did not affect basal levels of ROS (e.g., C522A, Fig. S5, Supporting information). Upon stimulation with 150 μM H_2O_2, ROS levels increased by 2.5-fold in HDFs expressing Flag-wt, whereas in HDFs expressing mutant C522/588/591A, ROS levels became saturated (Fig. 5A). These data suggest that in the presence of mutant C522/588/591A, ROS homeostasis is disturbed and HDFs become hypersensitive to oxidative stress. The basal levels of ROS were ~ 2.5-fold higher in Y259X HDF, compared to those expressing Flag-wt lamin A, and increased still further upon stimulation with H_2O_2 (Fig. 5A). In contrast, while HDF expressing progerin or R453W displayed basal levels of ROS that were ~ 1.5-fold higher than controls, upon stimulation with H_2O_2, ROS levels were only slightly elevated and did not exceed the levels observed following H_2O_2 stimulation in the controls (Fig. 5A). Importantly, pre-treatment of HDF with the ROS scavenger NAC abrogated the effects of H_2O_2 stimulation in all cases (Fig. 5A). We also investigated ROS in HDF from patients with X-linked EDMD, which are null for the inner nuclear membrane protein emerin and from patients with Greenberg Dysplasia, which are null for the inner nuclear membrane protein Lamin B receptor. We found that both basal levels and stimulated levels of ROS were identical to controls (data not shown). Taken together, these data suggest that hypersensitivity to oxidative stress is a phenotype that occurs specifically because of the loss of conserved cysteine residues in the lamin A tail or absence of lamin A, rather than general Nuclear Envelope defects or with disease-associated mutations in the *LMNA* tail domain. To confirm this finding, we also investigated the cellular

© 2011 The Authors
Aging Cell © 2011 Blackwell Publishing Ltd/Anatomical Society of Great Britain and Ireland

responses to mild H_2O_2 stimulation in HDF expressing progerin or R453W. We found that just like wild-type HDFs, these fibroblasts entered a reversible cell cycle arrest following stimulation with 150 μM H_2O_2 (Fig. 5B), and this treatment did not significantly increase the fraction of cells expressing SA-β-gal (Fig. 5C) or the percentage of dysmorphic nuclei (Fig. 5D). Taken together, these data confirm that the presence of functional lamin A is required for resilience to cellular ROS and that elimination of the conserved cysteine residues in the lamin A tail abrogates ROS-related functions of lamin A.

Previous studies have shown the hyperstimulation of ROS by treatment with 500 μM H_2O_2 produces a quantifiable molecular signature of up-regulated expression of transcription factors that can activate the expression of genes encoding antioxidant enzymes (p65, c-Fos, and Sp1), as well as the genes encoding the antioxidant enzymes themselves (manganese superoxide dismutase, CAT, and GST), prior to entry into a senescent state (Chaum *et al.*, 2009). We therefore used qPCR to quantify the expression of these genes in the presence or absence of mild (150 μM) H_2O_2 stimulation in fibroblasts expressing Flag-wt lamin A, C522/588/591A or progerin, or in lamin A null fibroblasts (Fig. 6). We found that the expression levels of all of the genes assessed were similar in HDF expressing Flag-wt lamin A and HDF expressing progerin (Fig. 6). In contrast, in the presence of C552/588/591A mutant or in the absence of lamin A, genes in the AP-1 (p65) and NFκB (c-Fos) family were both significantly up-regulated following H_2O_2 stimulation, although levels of expression of Sp-1 were similar to controls (Fig. 6). The likely downstream targets of oxidative stress–responsive transcription factors, including SOD, CAT and glutathione S-transferase were also all significantly higher in lamin A null HDF and HDF expressing C522/588/591A mutant following H_2O_2 stimulation compared to control and progerin expressing fibroblasts, suggesting that the antioxidant defence pathways were hyperactivated (Fig. 6). Of particular note was the level of activation of c-fos, which displayed a sixfold activation following H_2O_2 stimulation in the presence of C522/588/591A or in the absence of lamin A/C (Fig. 6). This level of activation was almost identical to the levels reported by Chaum *et al.* in response to chronic ROS stimulation. Thus, these data support our hypothesis that loss of lamin A or expression of C522/588/592A does lead to hypersensitivity to ROS stimulation and ROS intolerance.

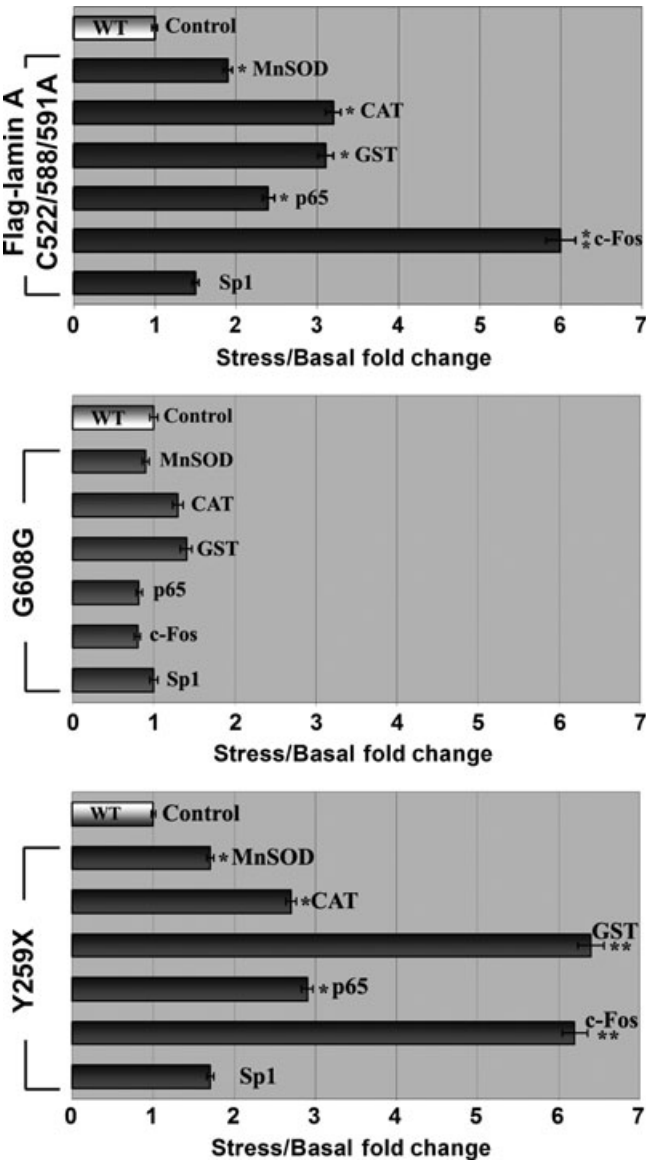


Fig. 6 C522/588/591A lamin A mutants induce expression of many stress-responsive genes. Flag-wt and C522/588/591A transfected human dermal fibroblasts (HDFs) as well as patient HDFs expressing progerin or that are null for lamin A/C (Y259X) were cultured in the presence (stress) or absence (basal) of 150 μM H_2O_2. Total RNA was isolated, and cDNA samples subjected to real-time qPCR using primers specific to phase II detoxification enzymes (manganese superoxide dismutase and catalase), glutathione enzyme (GST) and transcription factors NF-κB (p65), AP-1 (c-Fos), and Sp1. PCR for each sample was performed in triplicates in two independent experiments. Values for each sample were normalized to β-actin. Data were presented as fold change of the ratio between stress-induced and basal levels of gene expression relative to HDFs expressing Flag-wt lamin A, which is set at 1. *$P < 0.05$, **$P < 0.01$.

Decreasing cellular ROS abrogates the deleterious effects of mutant C522/588/591A

As HDFs expressing mutant C522/588/591A appear to be hypersensitive to oxidative stress, we predicted that the deleterious effects of this mutant on cell proliferation arose as a direct result of the increased cellular accumulation of ROS. To test this hypothesis, we investigated both nuclear morphology and cell proliferation in conditions that either increase or decrease cellular ROS. Initially, we analyzed nuclear morphology and SA-β-gal activity following stimulation with 150 μM H_2O_2. As expected, we did not observe a significant increase in dysmorphic nuclei or SA-β-gal expression (< 5%) in H_2O_2-treated Flag-wt HDFs (Fig. 7A,B). In contrast, H_2O_2-treated HDFs expressing C522/588/591A showed increases of 23% and 14% in dysmorphic nuclei and SA-β-gal expression, respectively, which were effectively prevented by NAC pre-treatment (Fig. 7A,B). Importantly, direct treatment of these fibroblasts with NAC (in the absence of H_2O_2) reduced basal levels of dysmorphic nuclei and SA-β-gal activity to levels similar to those observed in Flag-wt HDFs (Fig. 7A,B). These results suggest that the induction of dysmorphic nuclei and SIPS in HDFs expressing C522/588/591A results from higher levels of ROS accumulating in these cells, because they could be prevented by exogenous treatments with antioxidants.

Oxygen tension is another factor that can modulate cellular ROS levels (Parrinello *et al.*, 2003), and under standard culture conditions, oxygen tension is relatively high (20.6%). We therefore cultured cells under low (5%) oxygen tension to investigate whether this would ameliorate the deleterious effects of mutant C522/588/591A. Initially, we compared basal ROS levels in Flag-wt and the C522/C588/C591A mutant. As previously observed, under standard culture conditions, basal ROS levels were significantly higher in cells expressing the mutant compared to Flag-wt

© 2011 The Authors
Aging Cell © 2011 Blackwell Publishing Ltd/Anatomical Society of Great Britain and Ireland

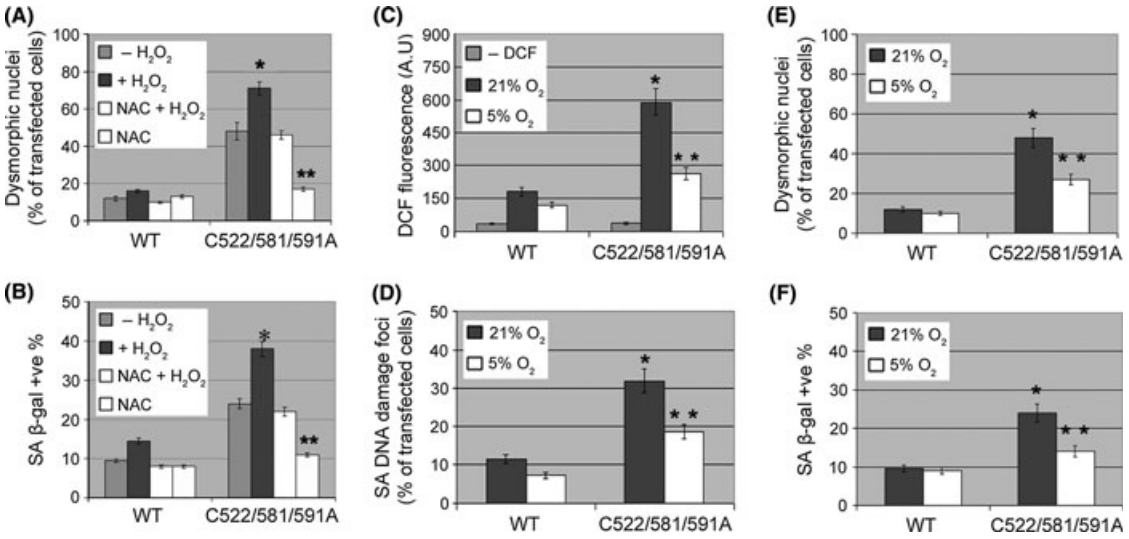


Fig. 7 Human dermal fibroblasts (HDFs) expressing C522/588/591A lamin A mutants show a lack of tolerance to mild oxidative stress. (A-B) Flag-wt or C522/588/591A expressing HDFs were left untreated or treated with 150 μM H_2O_2 in the presence or absence of 10 mM *N*-acetyl cysteine (NAC). Alternatively, transfected cultures were treated with 10 mM NAC in the absence of H_2O_2 stimulation. (A) The fraction of FLAG positive misshapen nuclei or (B) senescence-associated (SA)-β-gal-positive cells were determined 72 h after H_2O_2 stress. Fractions were calculated by scoring 300 cells on triplicate coverslips in three independent experiments. (C–F) Transfected HDFs were assessed under standard (20.6%) or low (5%) oxygen tension for basal ROS levels (C) and for fractions of FLAG positive nuclei showing either γH2A.X DNA damage foci (D), misshapen nuclei (E), or SA-β-gal-positive cells (F). Fractions were scored by counting 300 nuclei on triplicate coverslips from three independent experiments. Means ± SD are shown. **P* < 0.05 relative to untreated C522/588/591A HDFs (A,B), or Flag-wt HDFs at 21% O_2 (C–F). ***P* < 0.05 relative to untreated C522/588/591A HDFs (A,B), or Flag-cys HDFs at 21% O_2 (C–F).

lamin A (Fig. 7C). On the other hand, basal ROS levels in HDFs expressing the mutant were reduced by ~ 2.5-fold in 5% O_2 as compared to 20.6% O_2 (Fig. 7C). Similar reductions in cellular ROS were also observed following pre-treatment with NAC (Fig. 5). As ROS are major inducers of DNA damage, which is known to result in senescent arrest (Gorbunova *et al.*, 2002), we examined whether increased ROS levels in HDFs expressing the mutant were accompanied with the formation of DNA damage foci. We observed that when grown under standard oxygen tension, the fraction of cells displaying DNA damage foci was 3-fold greater in HDFs expressing C522/588/591A compared to Flag-wt lamin A. (Note the fraction of cells expressing DNA damage foci when transfected with single mutants were identical to controls – Fig. S5A, Supporting information). As expected, the fraction of HDFs displaying DNA damage foci declined significantly when they were grown under low oxygen tension (Fig. 7D). Similarly, the levels of both dysmorphic nuclei and SA-β-gal activity were also significantly decreased in HDFs expressing the mutant in 5% O_2 as compared to 20.6% O_2 conditions (Fig. 7E,F). Taken together, these results demonstrate that HDFs expressing C522/588/591A have a reduced tolerance to oxidative stress leading to a number of adverse effects including accumulation of ROS, ROS-induced DNA damage, and entry into premature stress-induced senescence. All of these adverse effects can be ameliorated, either by external ROS scavengers or by growth under low oxygen tension. These data support the hypothesis that loss of the conserved cysteine residues in the mammalian lamin A tail promotes senescence by rendering fibroblasts hypersensitive to ROS.

Discussion

Lamin A is essential for ROS tolerance

In this study, we highlight a novel function for lamin A in the cellular response to ROS stimulation. Lamin A is a target of irreversible oxidative modifications of conserved cysteine residues in its tail domain during cellular aging in vitro, which is correlated with decreased disulfide bond formation and alterations in nuclear morphology. We also show that HDFs normally respond to mild oxidative stresses, by forming disulfide bonds in lamin A and entering a state of temporary growth arrest. In contrast, in response to severe oxidative stress, lamin A disulfides do not form and HDFs enter a state of cellular senescence that is characterized by the appearance of dysmorphic nuclei. The adaptive response to mild oxidative stress is completely abrogated in HDF that are null for lamin A/C, which enter a state of cellular senescence that is characterized by the appearance of dysmorphic nuclei. This phenomenon is reversed by treating cells with a ROS chelator, suggesting that ROS is responsible for the appearance of dysmorphic nuclei. To investigate the role of conserved cysteine residues in lamin A function, we have created and characterized a novel panel of cysteine-alanine lamin A mutants, including a triple mutant (C552/588/591A) and a double mutant (C588/591A), which are unable to or have a greatly reduced ability to form disulfide bonds, and three single mutants C522A, C588A, and C591A all of which readily form disulfide bonds, albeit of differing molecular weights to wild-type lamin A. Of these mutants, only the triple mutant caused nuclear disorganization and entry into a state of cellular senescence in response to mild H_2O_2 stimulation, in a manner identical to lamin A null fibroblasts. This finding suggests that loss of the cysteine residues completely abrogates lamin A function in the adaptive cellular response to oxidative stress. Entry into a senescent state in the presence of the triple mutant or in the absence of lamin A is correlated with and appears to be caused by a dramatic increase in the levels of cellular ROS, because the deleterious effects of the mutant can be ameliorated either by treatment with ROS scavengers or by growth under low oxygen tension, and cells expressing the mutant or lacking lamin A display levels of activation of antioxidant genes in response to mild ROS stimulation, which are normally only observed under conditions of chronic oxygen stress (Chaum *et al.*, 2009). Our data are best explained by the hypothesis that in somatic cells, lamin A is essential to adapt to oxidative stress; when A-type lamins are gone, or

© 2011 The Authors
Aging Cell © 2011 Blackwell Publishing Ltd/Anatomical Society of Great Britain and Ireland

when crucial Cys residues are absent or irreversibly oxidized, cells cannot cope with even mild levels of oxidative stress and consequently enter the state of cellular senescence.

Cysteine modifications and cellular aging

Previous studies have shown that oxidative stress leads to cysteine oxidation of many proteins including lamins A/C (Eaton *et al.*, 2003). Oxidation of the conserved C-terminal cysteine residues in the lamin A tail during replicative senescence is correlated with an inability to form inter- and intramolecular disulfide bonds. Disulfide bond formation has been proposed to protect cells at various levels including protection of key cysteine residues from irreversible oxidation (Linke & Jakob, 2003). In the case of lamin A, disulfide bond formation under conditions of mild oxidative stress may protect its own cysteine residues from oxidative damage. Alternatively, it may also protect binding sites for stress-relevant partners that interact with the lamin A tail. These include SREBP (Lloyd *et al.*, 2002), PKCα (Tang *et al.*, 2000), 12(5)-lipoxygenase (Martelli *et al.*, 2002), c-fos (Ivorra *et al.*, 2006) and ERK (Gonzalez *et al.*,2008). Indeed, our observation that some of the single mutants (C522A and C588A) promote multiple intermolecular interactions supports the notion that the conserved cysteine residues form cross-linkages with several different proteins.

An alternative, non-exclusive explanation is that lamin A acts as a sink for ROS damage and this in itself protects less abundant proteins from oxidation. This has been reported previously for other abundant structural proteins such as actin, which appears to preferentially absorb ROS damage and acts as a redox sensor in the cytoplasm (Dalle-Donne *et al.*, 2003). Perhaps lamin A, because of its abundance and positioning within the nucleus, serves a similar purpose and at the point at which a critical proportion of conserved cysteine residues are oxidized, this promotes cellular senescence.

Protein oxidative damage is known to result in either a loss-of-function or a toxic gain-of-function (Linke & Jakob, 2003). Our results imply that oxidative damage to cysteine residues in the lamin A tail leads to a loss-of-function, because the cellular responses to ROS of the HDFs expressing the C522/588/591A mutant are identical to those of the Y259X lamin A null fibroblast cell line. This simple explanation, however, has to account for the dominant effects of the mutant over its endogenous wild-type counter part. The dominant effect of the mutant is presumably because lamin A is an obligate homo-dimer (Stuurman *et al.*, 1998), and therefore, in transfected HDFs, the C552/588/591A lamin A would become paired with its wild-type counterpart, in many instances. Parts of the lamin A tail are also essential for head-to-tail interactions between lamin A dimers during lamin filament assembly (Heitlinger *et al.*, 1992). Further work is needed to determine whether lamin filament assembly is disrupted by the triple mutant. We predict that during cellular aging, oxidation of the same cysteine residues would also lead to loss of these hierarchical interactions as is reflected in the accumulation of dysmorphic nuclei in senescent cells.

Why should loss of ROS-related lamin A function promote cellular senescence?

A-type lamins are ubiquitous and highly abundant nuclear proteins (Hutchison & Worman, 2004). Moreover, A-type lamins bind to and regulate a number of transcription factors that are pivotal to the processes of cell proliferation and cellular senescence. Specifically, lamin A has been shown to regulate a p53-dependent DNA damage response pathway (Liu *et al.*, 2005; Varela *et al.*, 2005), the pRb/E2F cell proliferation pathway (Markiewicz *et al.*, 2002; Johnson *et al.*, 2004; van Berlo *et al.*, 2005) and the AP1 pathway (Ivorra *et al.*, 2006; Gonzalez *et al.*, 2008). In particular, lamin A has been shown to be a key regulator of pRb function, and siRNA knockdown of lamin A in human cells has been shown to lead to impaired cell cycle progression and premature cell cycle arrest (Pekovic *et al.*, 2007). Thus, we propose that lamin A is essential for an adaptive response to oxidative stress in two ways: as a ROS 'sink', and because lamin A interacts with proteins that regulate cell cycle progression. We do not know whether binding to relevant partners is affected by the triple mutation, but speculate a potential effect on signaling via the Rb/LAP2α pathway (Markiewicz *et al.*, 2002; Dorner *et al.*, 2006) or via the ERK/fos pathway (Gonzalez *et al.*, 2008).

Conclusions

Previous studies have implied a role for either pre-lamin A accumulation or progerin in normal aging (McClintock *et al.*, 2006; Ukekawa *et al.*, 2007; Scaffidi & Misteli, 2008) and that these in concert with some other age-dependent mechanisms may be required for the observed adverse effects on nuclear morphology and cellular proliferation in aged cells (Kudlow & Kennedy, 2006). Our current findings suggest that oxidative damage to lamin A thiols has an important influence on cellular aging. We propose that oxidative damage to lamin A thiols may be the most important determinant of lamin A function in normal aging.

Experimental procedures

Cell culture and human dermal fibroblast strains

Human dermal fibroblast strains DD1 and DD2 were obtained from the foreskin of two healthy adolescent male donors. Human dermal fibroblasts were cultured in either atmospheric (20.6%) or low (5%) O_2 incubators in Dulbecco's modified Eagle's medium (DMEM; Invitrogen, Paisley, UK) supplemented with 10% fetal bovine serum (FBS) as previously described (Pekovic *et al.*, 2007). Human dermal fibroblasts were used between PDL 12-40 and harvested 3 days after subculture. Hutchinson Gilford Progeria Syndrome fibroblasts (AG06297) carrying classical G608G mutation in the *LMNA* gene were obtained from the Coriell Cell Repository. Human dermal fibroblasts from a patient with lethal fetal akinesis harboring a homozygous Y259X mutation in the *LMNA* gene were obtained as an autopsy sample after an informed consent and were a kind gift from Prof. Jos Broers. In addition, AD-EDMD HDFs carrying a R453W mutation in the *LMNA* gene, X-EDMD HDFs carrying a mutation in the *STA* gene, and HDFs from patients with Greenberg dysplasia carrying a mutation in the *LBR* gene were also obtained following informed consent.

H_2O_2 treatments

To induce oxidative stress, HDFs were cultured for 24 h in complete DMEM, serum-starved for 16 h and treated with hydrogen peroxide (H_2O_2, Sigma, Gillingham, UK) in serum-free, phenol-free DMEM for 1 h at indicated doses. For antioxidant treatments, HDFs were treated with free radical scavenger NAC (Sigma) in serum-free, phenol-free DMEM for 1 h at 10 mM. To induce SIPS, HDFs treated with 350 μM H_2O_2 were cultured for 3 days in complete DMEM, reseeded for 24 h, treated with a second dose of 350 μM H_2O_2, and cultured for another 3 days.

Immunocytochemistry and microscopy

Human dermal fibroblasts were fixed and permeabilized as previously described (Pekovic *et al.*, 2007). Primary antibodies are described in Table S1 (Supporting information). Secondary antibodies were donkey

© 2011 The Authors
Aging Cell © 2011 Blackwell Publishing Ltd/Anatomical Society of Great Britain and Ireland

anti-mouse and anti-rabbit IgG conjugated to rhodamine (TRITC) or fluorescein (FITC) (Stratech, Newmarket, UK). DNA was visualized by staining with 4,6-diamidino-2-phenyl-indole (DAPI) or Hoechst 33258 (Sigma). Intracellular ROS were detected by staining with carboxy-H_2DCFDA. Human dermal fibroblasts were imaged with Zeiss LSM510 META confocal microscope with LSM510 image browser software at ambient temperature, equipped with 40/1.3 oil-immersion lens and non-imaging photodetection device (photomultiplier tube) (Carl Zeiss MicroImaging, Welwyn Garden City, UK) using immersion oil (Immersol 518) as the imaging medium. A dynamic range adjustment was used to optimize the signal for the fluorophores, and any brightness and contrast adjustments were performed in Photoshop (Adobe). Phase contrast images were taken using Nikon Diaphot 300 fluorescence microscope attached to DXM1200 digital camera with Nikon ACT-1 imaging software.

Cell extraction

For whole cell extracts, cell pellets were lysed in ice-cold hypotonic buffer (10 mM Tris pH 7.4, 10 mM KCl, 3 mM $MgCl_2$, 0.1% Triton X-100), containing freshly added protease inhibitor cocktail and 100 units mL^{-1} RNAse-free DNAse I (Sigma) for 10 min on ice. For nuclear extracts, the above lysates were disrupted on ice in a Dounce homogenizer using a tight-fitting pestle and nuclei collected by centrifugation at 1000 *g* for 5 min at 4 °C prior to additional 10 min lysis in HB. All extracts were boiled in 2× sample buffer.

Gel electrophoresis and immunoblotting

One-dimensional SDS-PAGE and immunoblotting were performed as described previously (Pekovic *et al.*, 2007). Secondary antibodies were donkey anti-mouse or anti-rabbit IgG conjugated to horseradish peroxidase (HRP) (Jackson ImmunoResearch, Newmarket, UK). The enhanced chemiluminescence (ECL; Amersham, Amersham, UK) was used to detect HRP activity, and signals were visualized using Amersham Hyperfilm ECL in a Compact X4 Automatic X-ray Film Processor (Xograph Imaging Systems, Tedbury, UK). Densitometry of signals obtained for protein bands was performed using Image Gauge analysis software (FujiFilm, Bedford, UK).

Non-reducing/reducing SDS-PAGE

For detection of *in vivo* protein thiol status, protein extracts were prepared in the presence of alkylating agent NEM (Sigma) at 40 mM to prevent post-lysis thiol oxidation and boiled in non-reducing (minus DTT) or reducing (plus 200 mM DTT) 2× sample buffer as described previously (Benham *et al.*, 2000). Alternatively, extracts were prepared in the absence of NEM and air-exposed for 10 min prior to non-reducing/reducing SDS-PAGE.

SA-β-gal activity assay

Senescence-associated β-galactosidase (β-gal) activity was detected histochemically at pH 6 according to the manufacturer's instructions (cell signaling). The number of β-gal-positive cells (blue staining) was determined in 5–10 random microscopic fields from triplicate wells in three independent experiments.

Measurement of ROS production

Basal intracellular ROS were measured using 10 μM of cell-permeant non-fluorescent probe 5-,6-carboxy-2′,7′-dichlorodihydrofluorescein diacetate acetyl ester (carboxy-H_2DCFDA) (Molecular Probes, Victoria, AUS) in phenol-free, serum-free DMEM for 60 min at 37 °C. Oxidation of the probe to fluorescent form dichlorofluorescein (DCF) was traced using a fluorescence micro-plate reader (Fluoroskan Ascent; Lab Systems, Franklin Lakes, NJ, USA) with appropriate settings (excitation 485–95 nm; emission 520–25 nm). Readings were taken from triplicate wells and normalized to DNA content using 5 μg mL^{-1} Hoechst 33258 (excitation 360 nm; emission 450 nm). Alternatively, DCF fluorescence was traced using a FACSCalibur flow cytometer (Becton Dickinson, La Jolla, CA, USA) following the same conditions as above. Data were collected as histograms from 10 000 single-cell events, and median fluorescence intensity of FL1 peaks was analyzed using FlowJo software. To measure the rate of intracellular ROS production, cells were treated with 100 μM H_2O_2 during the last 20–30 min of incubation with carboxy-H_2DCFDA in serum-free, phenol-free DMEM. For antioxidant treatments, cells were incubated with 10 mM NAC for 1 h in phenol-free, serum-free DMEM containing carboxy-H_2DCFDA. As a background control, cells were incubated in phenol-free, serum-free DMEM without the probe.

Site-directed mutagenesis and transfections

The pSVK3 plasmid containing full-length human pre-lamin A cDNA fused with an N-terminal FLAG tag was a kind gift from Prof. Howard Worman. Flag-lamin A cDNAs harboring either single (C522A, C588A, and C591A), double (C588/C591A) or triple (C522A/C588A/C591A) or cysteine-to-alanine mutations were produced by PCR using QuickChange II Site-Directed Mutagenesis Kit (Stratagene, Huntingdon, UK). Primer sequence design and PCR cycling parameters were performed according to the manufacturer's guidelines. Four pairs of mutagenic lamin A primer sequences carrying the desired cys-to-ala substitutions are shown in Table S2 (Supporting information). Transformation was performed into *Escherichi coli* strain XL1-Blue, and plasmids were purified using Qiagen MidiPrep DNA purification kit. All mutant constructs were sequenced to verify the presence of desired mutations and the absence of any extraneous mutations. DNA constructs were transfected into HDFs using Nucleofector technology (Amaxa, Paisley, UK). Transfection efficiency was ~ 40%.

MALDI-TOF/TOF peptide mass fingerprinting

Nuclear extracts were prepared in the presence of 40 mM NEM and subjected to reducing SDS-PAGE. Gels were stained with Coomassie Brilliant Blue dye, protein bands excised, and subjected to reductive alkylation with 10 mM DTT and 100 mM iodoacetamide (IAM) prior to ProGest trypsin digestion. The resulting peptides were analyzed by matrix-assisted laser desorption ionization time-of-flight/time-of-flight mass spectrometry (4800 Plus MALDI-TOF/TOF Analyser and top 10 peptides from the initial MS spectra were selected for MS/MS sequencing. De-isotoped and calibrated spectra were used to generate lists of peptide mass peaks that were submitted to Mascot database search engine and lamin A/C identification obtained by matching multiple peptides to the corresponding entry within the NCBI database (> 80% sequence coverage). Modified cysteine-containing peptides (including peptides with one missed cleavage site) of lamin A/C were searched in Mascot database by specifying alkylation with NEM (125 Da) and/or IAM (57 Da) and oxidative modifications including oxidation to sulfenic acid (16 Da), di-oxidation to sulfinic acid (32 Da), and tri-oxidation to sulfonic acid (48 Da).

cDNA synthesis and real-time qPCR

Flag-wt and Flag-cys lamin A transfected HDFs were cultured in complete DMEM or treated for 1 h with 200 μM H_2O_2 in serum-free, phenol-free

© 2011 The Authors
Aging Cell © 2011 Blackwell Publishing Ltd/Anatomical Society of Great Britain and Ireland

DMEM. Total RNA was isolated from cells using RNeasy Mini Kit (Qiagen) according to the manufacturer's guidelines. 1 μg of each RNA sample was synthesized into cDNA using Promega Reverse Transcription System. cDNA samples were subjected to SYBR Green-based real-time qPCR in an ABI 7500 Fast Real-Time PCR System (Applied Biosystems) using primers for β-actin and six stress response genes shown in Table S3 (Supporting information). cDNA samples containing no reverse transcription were used as negative controls for contaminating genomic DNA. The conditions for PCR amplifications were 40 cycles at 95 °C for 10 s and at 60 °C for 30 s. PCR for each sample was performed in triplicates in two independent experiments. Values for each sample were recorded by 7500 Fast System Software and normalized to β-actin signals, which did not show any significant variation between samples relative to the cDNA input. Data were presented as a fold change of the ratio between stress-induced and basal levels of gene expression.

Statistical analyses

Data were evaluated using independent *t*-test or χ^2 test as indicated. Results are presented as means ± SD. from at least three independent experiments. Differences were considered significant at the value of $P < 0.05$.

Acknowledgments

We thank Joanne Robson for the help with mass spec analyses and Dr Stefan Przyborski for the use of 5% O_2 incubator. This work was supported by the grants from The Association for International Cancer Research (CJH), the Muscular Dystrophy Campaign (CJH), and the EURO-laminopathies FP6 program (CJH).

Author contributions

Vanja Pekovic, Ian Gibbs-Seymour, Ewa Markiewicz, and Fahad Al Zhogaibi all performed experimental work contributing to this study. Adam Benham, Robert Edwards, and Thomas von Zlinicki all contributed to the design of experiments in this study. Manfred Wehnert contributed patient cell lines and contributed to the design of experiments. Chris Hutchison supervised the research and wrote the manuscript.

References

d'Adda di Fagagna F, Reaper PM, Clay-Farrace L, Fiegler H, Carr P, Von Zglinicki T, Saretzki G, Carter NP, Jackson SP (2003) A DNA damage checkpoint response in telomere-initiated senescence. *Nature* **426**, 194–198.

Benham AM, Cabibbo A, Fassio A, Bulleid N, Sitia R, Braakman I (2000) The CXXCXXC motif determines the folding, structure and stability of human Ero1-Lα. *EMBO J.* **19**, 4493–4502.

Ben-Harush K, Weisel N, Frenkiel-Krispin D, Moeller D, Soreg E, Aebi U, Herrmann H, Gruenbaum Y, Medalia O (2009) The supramolecular organization of the *C. elegans* nuclear lamin filament. *J. Mol. Biol.* **386**, 1392–13402.

van Berlo JH, Voncken JW, Kubben N, Broers JL, Duisters R, van Leeuwen RE, Crijns HJ, Ramaekers FC, Hutchison CJ, Pinto YM (2005) A-type lamins are essential for TGF-beta1 induced PP2A to dephosphorylate transcription factors. *Hum. Mol. Genet.* **14**, 2839–2849.

Bridger JM, Kill IR (2004) Aging of Hutchinson-Gilford progeria syndrome fibroblasts is characterised by hyperproliferation and increased apoptosis. *Exp. Gerontol.* **39**, 717–724.

Broers JL, Ramaekers FC, Bonne G, Yaou RB, Hutchison CJ (2006) Nuclear lamins: laminopathies and their role in premature ageing. *Physiol. Rev.* **86**, 967–1008.

Campisi J (2005) Senescent cells, tumor suppression, and organismal aging: good citizens, bad neighbors. *Cell* **120**, 513–522.

Candelario J, Sudhakar S, Navarro S, Reddy S, Comai L (2008) Perturbation of wild-type lamin A metabolism results in a progeroid phenotype. *Aging Cell* **7**, 355–367.

Cao K, Capell BC, Erdos MR, Djabali K, Collins FS (2007) A lamin A protein isoform overexpressed in Hutchinson-Gilford progeria syndrome interferes with mitosis in progeria and normal cells. *Proc. Natl Acad. Sci. USA* **104**, 4949–4954.

Chaum E, Yin J, Yang H, Thomas F, Lang JC (2009) Quantitative AP-1 gene regulation by oxidative stress in the human retinal pigment epithelium. *J. Cell. Biochem.* **108**, 1280–1291.

Dalle-Donne I, Rossi R, Giustanni D, Colombo R, Milzani A (2003) Actin S-glutathionylation: evidence against thiol-disulphide exchange mechanisms. *Free Radic. Biol. Med.* **35**, 1185–1193.

Davies KJ (1999) The broad spectrum of responses to oxidants in proliferating cells: a new paradigm for oxidative stress. *IUBMB Life* **48**, 41–47.

Dechat T, Shimi T, Adam SA, Rusinol AE, Andres DA, Spielmann HP, Sinensky MS, Goldman RD (2007) Alterations in mitosis and cell cycle progression caused by a mutant lamin A known to accelerate human aging. *Proc. Natl Acad. Sci. USA* **104**, 4955–4960.

Dorner D, Vlcek S, Foeger N, Gajewski N, Makolm C, Gotzmann J, Hutchison CJ, Foisner R (2006) Lamina-associated polypeptide 2 alpha regulates cell cycle progression and differentiation via the retinoblstoma-E2F pathway. *J. Cell Biol.* **173**, 83–93.

Duque G, Rivas D (2006) Age-related changes in lamin A/C expression in the osteoarticular system: laminopathies as a potential new aging mechanism. *Mech. Ageing Dev.* **127**, 378–383.

Eaton P (2006) Protein thiol oxidation in health and disease: techniques for measuring disulfides and related modifications in complex protein mixtures. *Free Radic. Biol. Med.* **40**, 1889–1899.

Eaton P, Jones ME, McGregor E, Dunn MJ, Leeds N, Byers HL, Leung KY, Ward MA, Pratt JR, Shattock MJ (2003) Reversible cysteine-targeted oxidation of protein during renal oxidative stress. *J. Am. Soc. Neprhol.* **14**, 290–296.

Eruslanov E, Kusmartsev S (2010) Identification of ROS using oxidized DCFDA and flow-cytometry. *Methods Mol Biol.* **594**, 57–72.

Espada J, Varela I, Flores I, Ugalde AP, Cadinanos J, Pendas AM, Stewart CL, Tryggvason K, Blasco MA, Freije JM, Lopez-Otin C (2008) Nuclear envelope defects cause stem cell dysfunction in premature-aging mice. *J. Cell Biol.* **181**, 27–35.

Friguet B (2006) Oxidized protein oxidation and repair during ageing and oxidative stress. *FEBS Lett.* **580**, 2910–2916.

Goldman RD, Shumaker DK, Erdos MR, Eriksson M, Goldman AE, Gordon LB, Gruenbaum Y, Khuon S, Mendez M, Varga R, Collins FS (2004) Accumulation of mutant lamin A causes progressive changes in nuclear architecture in Hutchinson-Gilford progeria syndrome. *Proc. Natl Acad. Sci. USA* **101**, 8963–8968.

Gonzalez JM, Navarro-Puche A, Casar B, Crespo P, Andres V (2008) Fast regulation of AP-1 activity through interaction of lamin A/C, ERK1/2, and c-Fos at the nuclear envelope. *J. Cell Biol.* **183**, 653–666.

Gorbunova V, Seluanov A, Pereira-Smith OM (2002) Expression of human telomerase (hTERT) does not prevent stress-induced senescence in normal human fibroblasts but protects the cells from stress-induced apoptosis and necrosis. *J. Biol. Chem.* **277**, 38540–38549.

Haddad JJ (2002) Antioxidant and prooxidant mechanisms in the regulation of redox-sensitive transcription factors. *Cell. Signal.* **14**, 879–897.

Haithcock E, Dayani Y, Neufeld E, Zahand AJ, Feinstein N, Mattout A, Gruenbaum Y, Liu J (2005) Age-related changes of nuclear architecture in *Caenorhabditis elegans*. *Proc. Natl Acad. Sci. USA* **102**, 16690–16695.

Harborth J, Elbashir SM, Bechert K, Tuschl T, Weber K (2001) Identification of essential genes in cultured mammalian cells using small interfering RNAs. *J Cell Sci.* **114**(**Pt 24**), 4557–4565.

Harman D (1956) Aging: a theory based on free radical and radiation chemistry. *J. Gerontol.* **11**, 298–300.

Heitlinger E, Peter M, Lustig A, Villiger W, Nigg EA, Aebi U (1992) The role of the head and tail domain in lamin structure and assembly: analysis of bacterially expressed chicken lamin A and truncated B2 lamins. *J. Struct. Biol.* **108**, 74–89.

Huang S, Risques RA, Martin GM, Rabinovitch PS, Oshima J (2008) Accelerated telomere shortening and replicative senescence in human fibroblasts overexpressing mutant and wild-type lamin A. *Exp. Cell Res.* **314**, 82–91.

Hutchison CJ, Worman HJ (2004) A-type lamins: guardians of the soma? *Nat. Cell Biol.* **6**, 1062–1067.

© 2011 The Authors
Aging Cell © 2011 Blackwell Publishing Ltd/Anatomical Society of Great Britain and Ireland

Ivorra C, Kubicek M, Gonzalez JM, Sanz-Gonzalez SM, Alvarez-Barrientos A, O'Connor JE, Burke B, Andres V (2006) A mechanism of AP-1 suppression through interaction of c-Fos with lamin A/C. *Genes Dev.* **20**, 307–320.

Johnson BR, Nitta RT, Frock RL, Mounkes L, Barbie DA, Stewart CL, Harlow E, Kennedy BK (2004) A-type lamins regulate retinoblastoma protein function by promoting subnuclear localization and preventing proteasomal degradation. *Proc. Natl Acad. Sci. USA* **101**, 9677–9682.

Krimm I, Ostlund C, Gilquin B, Couprie J, Hossenlopp P, Mornon JP, Bonne G, Courvalin JC, Worman HJ, Zinn-Justin S (2002) The Ig-like structure of the C-terminal domain of lamin A/C, mutated in muscular dystrophies, cardiomyopathy, and partial lipodystrophy. *Structure* **10**, 811–823.

Kudlow BA, Kennedy BK (2006) Ageing: progeria and the lamin connection. *Curr. Biol.* **16**, 652–654.

Linke K, Jakob U (2003) Not every disulfide lasts for ever: disulfide bond formation as a redox switch. *Antioxid. Redox Signal.* **5**, 425–434.

Liu B, Wang J, Chan KM, Tjia WM, Deng W, Guan X, Huang JD, Li KM, Chau PY, Chen DJ, Pei D, Pendas AM, Cadmanos J, Lopez-Otin C, Tse HF, Hutchison CJ, Chen J, Cao Y, Cheah KS, Tryggvason K, Zhou Z (2005) Genomic instability in laminopathy-based premature aging. *Nat. Med.* **11**, 780–785.

Lloyd DJ, Trembath RC, Shackleton S (2002) A novel interaction between lamin A and SREBP1: implications for partial lipodystrophy and other laminopathies. *Hum. Mol. Genet.* **11**, 769–777.

Markiewicz E, Dechat T, Foisner R, Quinlan RA, Hutchison CJ (2002) Lamin A/C binding protein LAP2alpha is required for nuclear anchorage of retinoblastoma protein. *Mol. Biol. Cell*, **13**, 4401–4413.

Martelli AM, Bortul R, Tabellini G, Faenza I, Cappellini A, Bareggi R, Manzoli L, Cocco L (2002) Molecular characterization of protein kinase C-alpha binding to lamin A. *J. Cell. Biochem.* **86**, 320–330.

McClintock D, Gordon LB, Djabali K (2006) Hutchinson-Gilford progeria mutant lamin A primarily targets human vascular cells as detected by an anti-Lamin A G608G antibody. *Proc. Natl Acad. Sci. USA* **103**, 2154–2159.

Muchir A, van Engelen BG, Lammens M, Mislow JM, McNally E, Schwartz K, Bonne G (2003) Nuclear envelope alterations in fibroblasts from LGMD1B patients carrying nonsense Y259X heterozygous or homozygous mutation in lamin A/C gene. *Exp. Cell Res.* **291**, 352–362.

Navarro CL, De Sandre-Giovannoli A, Bernard R, Boccaccio I, Boyer A, Genevieve D, Hadj-Rabia S, Gaudy-Marqueste C, Smitt HS, Vabres P *et al.* (2004) Lamin A and ZMPSTE24 (FACE-1) defects cause nuclear disorganization and identify restrictive dermopathy as a lethal neonatal laminopathy. *Hum. Mol. Genet.* **13**, 2493–2503.

Parrinello S, Samper E, Krtolica A, Goldstein J, Melov S, Campisi J (2003) Oxygen sensitivity severely limits the replicative lifespan of murine fibroblasts. *Nat. Cell Biol.* **5**, 741–747.

Pekovic V, Hutchison CJ (2008) Adult stem cell maintenance and tissue regeneration in the ageing context: the role for A-type lamins as intrinsic modulators of ageing in adult stem cells and their niches. *J. Anat.* **213**, 5–25.

Pekovic V, Harborth J, Broers JL, Ramaekers FC, van Engelen B, Lammens M, von Zglinicki T, Foisner R, Hutchison C, Markiewicz E (2007) Nucleoplasmic LAP2α-lamin A complexes are required to maintain a proliferative state in human fibroblasts. *J. Cell Biol.* **176**, 163–172.

Pekovic V, Harborth J, Broers JL, Ramaekers FC, van Engelen B, Lammens M, von Zglinicki T, Foisner R, Hutchison C, Markiewicz E (2006) Nucleoplasmic LAP2 alpha-lamin A complexes are required to maintain a proliferative state in human fibroblasts. *J. Cell Biol.* **176**, 163–172.

Reddy KL, Zullo JM, Bertolino E, Singh H (2008) Transcriptional repression mediated by repositioning of genes to the nuclear lamina. *Nature* **452**, 243–247.

Rusinol AE, Sinensky MS (2006) Farnesylated lamins, progeroid syndromes and farnesyl transferase inhibitors. *J. Cell Sci.* **119**, 3265–3272.

Scaffidi P, Misteli T (2008) Lamin A-dependent misregulation of adult stem cells associated with accelerated ageing. *Nat. Cell Biol.* **10**, 452–459.

Stewart CL, Kozlov S, Fong LG, Young SG (2007) Mouse models of the laminopathies. *Exp. Cell Res.* **313**, 2144–2156.

Stuurman N, Heins S, Aebi U (1998) Nuclear lamins: their structure, assembly, and interactions. *J. Struct. Biol.* **122**, 42–66.

Tang K, Finley Jr RL, Nie D, Honn KV (2000) Identification of 12-lipoxygenase interaction with cellular proteins by yeast two-hybrid screening. *Biochemistry* **39**, 3185–3191.

Toussaint O, Medrano EE, von Zglinicki T (2000) Cellular and molecular mechanisms of stress-induced premature senescence (SIPS) of human diploid fibroblasts and melanocytes. *Exp. Gerontol.* **35**, 927–945.

Ukekawa R, Miki K, Fujii M, Hirano H, Ayusawa D (2007) Accumulation of multiple forms of lamin A with down-regulation of FACE-1 suppresses growth in senescent human cells. *Genes Cells* **12**, 397–406.

Varela I, Cadinanos J, Pendas AM, Gutierrez-Fernandez A, Folgueras AR, Sanchez LM, Zhou Z, Rodriguez FJ, Stewart CL, Vega JA, Tryggvason K, Freije JM, Lopez-Otin C (2005) Accelerated ageing in mice deficient in Zmpste24 protease is linked to p53 signalling activation. *Nature* **437**, 564–568.

Vergenes L, Pekerfly MN, Bergo MO, Young SG, Reve K (2004) Lamin B1 is required for mouse development and nuclear integrity. *Proc. Natl. Acad. Sci. USA* **101**, 10428–10433.

Worman HJ, Bonne G (2007) Laminopathies: a wide spectrum of human diseases. *Exp. Cell Res.* **313**, 2121–2133.

von Zglinicki T, Petrie J, Kirkwood TB (2003) Telomere-driven replicative senescence is a stress response. *Nat. Biotechol.* **21**, 229–230.

von Zglinicki T, Saretzki G, Ladhoff J, d'Adda di Fagagna F, Jackson SP (2005) Human cell senescence as a DNA damage response. *Mech. Ageing Dev.* **126**, 111–117.

Supporting Information

Additional supporting information may be found in the online version of this article:

Fig. S1 Multiple sequence alignments of C-termini of human lamins.

Fig. S2 Multiple sequence alignments of lamin A tail in vertebrates.

Fig. S3 Mass spectrometry analysis of lamin A in young and senescent fibroblasts.

Fig. S4 HDFs induced to senesce by exposure to high levels of H2O2 show dysmorphic nuclei and SA-β-gal activation.

Fig. S5 HDFs containing lamin A C522A mutant show no significant change in levels of ROS or DNA damage.

Table S1 Primary antibodies used in this study.

Table S2 Primer sequences used for site-directed mutagenesis.

Table S3 Primer sequences used for real-time qPCR.

As a service to our authors and readers, this journal provides supporting information supplied by the authors. Such materials are peer-reviewed and may be re-organized for online delivery, but are not copy-edited or typeset. Technical support issues arising from supporting information (other than missing files) should be addressed to the authors.

© 2011 The Authors
Aging Cell © 2011 Blackwell Publishing Ltd/Anatomical Society of Great Britain and Ireland